Hyperpolarization induced by vasoactive substances in intact guinea-pig endocardial endothelial cells

K. Manabe, H. Ito, H. Matsuda and A. Noma*

Department of Physiology, Faculty of Medicine, Kyushu University, Fukuoka 812, Japan

1. The responses of guinea-pig endocardial endothelial (EE) cells to various vasoactive substances were investigated in either the small tissue preparation or freshly isolated cells using the patch clamp technique.

2. The mean resting potential of the EE cell was −44 mV in the small tissue preparation, and applications of ATP, ADP, AMP, adenosine, histamine and substance P induced transient hyperpolarizations of −22, −21, −9, −10, −23 and −15 mV, respectively. The membrane potential of EE cells failed to respond to acetylcholine, bradykinin, thrombin, atrial natriuretic peptide, vasopressin and serotonin.

3. The whole-cell voltage clamp of dissociated cells revealed a transient increase of K^+ conductance underlying the ATP and histamine responses. The agonist-induced current showed no time-dependent change during voltage steps. The response was prevented by adding 10 mM EGTA to the pipette solution.

4. In the cell-attached single channel recordings, ATP induced transient K^+ channel activities having a slope conductance of 34 pS. In inside-out patches, similar K^+ channels were activated by applying Ca^{2+} of more than 0·1 μM.

5. These findings are consistent with the idea that the Ca^{2+}-dependent K^+ channel is involved in the hyperpolarizing response of EE cells, as described in vascular endothelial cells.

It has recently been demonstrated that endocardial endothelial (EE) cells play an important role in modulating the performance of the subjacent cardiac muscle (Meulemans, Sipido, Sys & Brutsaert, 1988; Shah, Andries, Meulemans & Brutsaert, 1989*a*; Schoemaker, Meulemans, Andries & Brutsaert, 1990; Wang & Morgan, 1992). The EE cells may release some unknown chemical messengers such as myocardium relaxing factor (Brutsaert, 1989; Brutsaert & Andries, 1992) and contraction-prolonging factor (Smith, Shah & Lewis, 1991; Mebazaa *et al.* 1993) in response to various vasoactive substances circulating in the superfusing blood. It is also suggested that the endocardium may maintain the interstitial K^+ concentration in the heart at lower levels than that in the plasma, which has been defined as 'electrochemical control' (Brutsaert, 1989; see also the accompanying paper, Manabe, Ito, Matsuda, Noma & Shibata, 1995). However, electrophysiology of EE cells is still quite limited when compared with that of vascular endothelial cells (Newby & Henderson, 1990; Takeda & Klepper, 1990; Ito, Matsuda & Noma, 1993). Since most cardiac myocytes are separated from blood by microvascular coronary endothelial cells, the comparison of the EE cells with the coronary endothelial cells is interesting (Daut, Mehrke, Nees & Newman, 1988; Mehrke & Daut, 1990; Mehrke, Pohl & Daut, 1991; Chen & Cheung, 1992).

The present study aims to investigate the response of the EE cells to various vasoactive substances. For this purpose, we used mainly intact EE cells or freshly isolated cells to minimize the complications arising from using cultured cells (see also Chen & Cheung, 1992; Yamamoto, Chen, Miwa & Suzuki, 1992; Marchenko & Sage, 1993; Ito *et al.* 1993). The responsiveness of the cultured endothelial cells might be altered either by the enzymatic treatment for isolation or by the variation of the culture medium (Tracey & Peach, 1992). We applied various vasoactive substances to intact EE cells and demonstrate that EE cells possess a different set of receptors compared with those reported in the endothelial cells from various vascular beds. Application of ATP, ADP, AMP, adenosine, histamine or substance P induces transient hyperpolarizations, while acetylcholine (ACh), bradykinin and thrombin are ineffective. The activation of Ca^{2+}-dependent K^+ channels, which has been demonstrated to underlie the hyperpolarizing responses of the aortic and coronary

* To whom correspondence should be sent at the following address: Department of Physiology, Faculty of Medicine, Kyoto University, Kyoto 606, Japan.

endothelial cells (for review see Takeda & Klepper, 1990), is examined on both the single channel and whole-cell current levels.

METHODS

Preparation

Adult guinea-pigs (200–300 g) were anaesthetized with intraperitoneal injections of sodium pentobarbitone (90 mg kg^{-1}). The heart was dissected out and perfused with nominally Ca^{2+}-free Tyrode solution through the coronary artery on a Langendorff apparatus and was used for preparing both the small tissue and the isolated cell preparations.

Small tissue preparation (*in situ* endothelium). The atrium or ventricle was opened. In order to improve the success ratio of forming a gigaseal, the tissue surface was treated with protease (10 mg dl^{-1} dissolved in nominally Ca^{2+}-free Tyrode solution; Sigma Chemical Co., St Louis, MO, USA) for 5 min. The heart was stored in a high-K^+ storage solution at room temperature (20–25 °C) and was used within a day. A small tissue specimen of the atrium, ventricle or valves, approximately 1·0 × 1·0 mm in size, was excised and fixed on the bottom of a recording chamber with the luminal side up by pressing it with two tungsten wires.

Isolated cell preparations. Two types of isolated EE cell preparations were used. The first preparation is one in which the cells were dissociated with the stream method and the second one in which the cells were obtained with the stamp method.

To dissociate EE cells with the stream method, the dissected heart was treated with collagenase (3·5–4·0 mg dl^{-1} in nominally Ca^{2+}-free Tyrode solution; Yakult, Tokyo, Japan) for 10 min. After washing out the collagenase by perfusing the heart with the high-K^+ storage solution, EE cells were dissociated by applying a gentle stream of the storage solution to the endocardial surface of the atrial tissue.

To record single channel current from the abluminal membrane, EE cells isolated with the stamp method were used. A poly-L-lysine-coated (0·5%; Sigma) coverslip was attached to the atrial endocardium and then removed from the tissue accompanied by EE cells which were attached to the glass surface. This method is essentially the same as that used in cultured endothelial cells (Colden-Stanfield, Cramer & Gallin, 1992). The isolated cells, with their abluminal membranes up, were present showing the cobblestone-like appearance of two to fifteen non-overlapping cells (see the accompanying paper, Manabe *et al.* 1995). The isolation of the EE cells was facilitated by an additional treatment with collagenase (5 mg dl^{-1}) for 3–5 min. The coverslip was put into the recording chamber which was mounted on the inverted microscope.

Solutions

The control Tyrode solution contained (mM): 140 NaCl, 5·4 KCl, 0·5 $MgCl_2$, 0·33 NaH_2PO_4, 1·8 $CaCl_2$, 5·5 glucose and 5 Hepes–NaOH, pH 7·4. The nominally Ca^{2+}-free Tyrode solution was made simply by omitting $CaCl_2$. The composition of the high-K^+ storage solution was (mM): 30 KCl, 70 potassium glutamate, 10 KH_2PO_4, 1 $MgCl_2$, 20 taurine, 0·3 ethyleneglycol-bis-(β-aminoethylether) *N,N,N′,N′*-tetraacetic acid (EGTA; Sigma), 10 glucose and 10 Hepes (pH 7·3, titrated with KOH).

The composition of the pipette solution used for the conventional whole-cell voltage clamp experiments was (mM): 90 potassium aspartate, 20 KCl, 10 NaCl, 5 Mg-ATP, 0·1 GTP, 0·05 EGTA and 5 Hepes–KOH (pH 7·2). Essentially the same ionic composition was used for the nystatin-perforated whole-cell patch recordings except that 1 mM $CaCl_2$ was used in place of EGTA. Stock solutions of nystatin (25 mg ml^{-1}; Sigma) were prepared daily by dissolving in dimethylsulphoxide (DMSO; Ishizu Pharmaceutical Co. Ltd, Osaka, Japan) and were added to the pipette solution to obtain a final concentration of 20–100 μg ml^{-1}. The pipette solution used for single channel recording was a high-K^+ solution containing (mM): 150 KCl, 1 $CaCl_2$ and 5 Hepes–KOH, pH 7·4. In the inside-out patch recordings, the free Ca^{2+} concentration of the bath solution was buffered by 0·3 or 1·0 mM EGTA. The concentration of free Ca^{2+} was calculated by a computer program (Fabiato & Fabiato, 1979; Tsien & Rink, 1980).

The following vasoactive substances were used in this study: atrial natriuretic peptide (ANP) and substance P (both from Peptide Institute Inc., Osaka, Japan); ATP, ADP, AMP, adenosine, histamine, ACh, bradykinin, serotonin, vasopressin and thrombin (all from Sigma). These were added to the control Tyrode solution, and applied to the cell by switching the perfusates at the inlet of the recording chamber. A rapid application of the agonist was difficult because a slight vibration of the bathing solution could dislodge the patch electrode from the intact EE cells.

Recordings

The small tissue preparation was used to record either the membrane potential or single channel current of luminal membrane. The EE cells dissociated with the stream method were used for conventional whole-cell voltage clamp. The cells obtained with the stamp method were used to record the resting potential or single channel current of abluminal membrane. All patch clamp recordings (Hamill, Marty, Neher, Sakmann & Sigworth, 1981) were performed using a patch clamp amplifier (EPC-7 List Electronic, Darmstadt, Germany).

The tissue and cell preparations were allowed to equilibrate for 5–20 min in the control Tyrode solution before recording. The experiments using the small tissue preparation were performed using the following recording method. Under a stereomicroscope, the electrode tip was slowly moved down towards the tissue surface while monitoring the electrode resistance. The attachment of the electrode tip to the luminal membrane of EE cells was recognized from a slight but quick increase of the electrode resistance. The application of a negative pressure of 10–50 cmH_2O to the interior of the electrode facilitated a tight-seal formation (10–100 GΩ). Although we carefully cut off as much of the underlying myocardium as possible, even a slight movement of the remaining myocardium dislodged the electrode tip because the thickness of EE cells is less than 1 μm (Brutsaert & Andries, 1992).

The nystatin-perforated-patch recording technique (Mistry & Hablitz, 1990) was applied to measure the membrane potential in the small tissue preparation and the cells obtained with the stamp method. The electrode was filled with the nystatin-containing solution and gentle suction was used to achieve a gigaseal. To monitor the perforation of the patch membrane, hyperpolarizing pulses of 5 mV were applied at a pipette potential of −20 mV. The access resistance gradually decreased within 1–5 min after the tight-seal formation, and the membrane potential recorded in the current clamp mode reached a steady value. Only preparations and cells exhibiting stable

resting potentials were used in the present study. The success ratio in this method was 5–20%.

Conventional whole-cell voltage clamp recording was obtained from the cells dissociated with the stream method. The membrane capacitance (C_m), measured from the current jump on inverting the slope of the ramp pulses (±1 or 2 $V s^{-1}$), was 7·4 ± 0·5 ($n = 25$; mean ± S.E.M.), 13·4 ± 0·6 ($n = 23$) and 19·8 ± 1·0 pF ($n = 18$) for single, paired and triplet cells, respectively. Since the membrane capacitance was roughly proportional to the number of cells with a slope of 6·5 pF $cell^{-1}$, we assumed that the cells were well electrically coupled via gap junctions, and used data obtained from clusters of one to three cells. Voltage clamp recording from paired or triplet cells was more stable than from single cells. The use of cell clusters may also be justified by the space constant of 250–550 μm in the one-dimensional cable model used for the monolayer of the coronary endothelial cells (Daut *et al.* 1988) and by the direct measurement of the electrical coupling within the two to eight cell cluster of the cultured endothelial cells (Mendelowitz, Bacal & Kunze, 1992). Rupturing the patch membrane using strong suction was without success in the small tissue preparation and the cells obtained with the stamp method.

Patch electrodes were made from 1·5 mm o.d. glass capillaries and were fire polished before use. In single channel recordings, they were coated near their tips with silicon to reduce the stray capacitance. The electrode resistance was 10–12 MΩ for single channel recording, 25–35 MΩ for conventional whole-cell voltage clamp and 2–6 MΩ for nystatin-perforated membrane potential recording when filled with each pipette solution. The recording bath was grounded through an agar–Tyrode and Ag–AgCl bridge. In both the conventional and nystatin-perforated whole-cell recordings, membrane potentials were corrected for the liquid junction potential (−8 mV) at the tip of the pipette in the control Tyrode solution.

All experiments were performed at 32–34 °C.

Data analysis

The current and voltage signals were recorded on a videotape using a PCM converter (RP-880, NF, Yokohama, Japan) for subsequent computer analysis (PC-98XA or XL, NEC, Tokyo, Japan). The whole-cell current–voltage (I–V) relationships were measured by applying either square or ramp pulses from a holding potential of −50 mV. Ramp pulses were ±100 mV in amplitude and ±1 or 2 $V s^{-1}$ in slope. I–V relationships were obtained from the descending limb of the ramp pulses after correcting for the capacitive current. The slope conductance and reversal potential were determined by calculating a regression line over an appropriate small segment of recordings.

The single channel currents were filtered using a four-pole Bessel-type low-pass filter (E-3201A, NF) with a −3 dB corner frequency of 500 Hz and sampled every 1 ms. The amplitude of a unitary current was measured as the distance between two horizontal lines set by eye at the closed and open levels. In several experiments, the variance–mean analysis method developed by Patlak was used (Patlak, 1988). There was no marked difference in the unitary amplitudes obtained from these two methods. The open probability (P_o) of the channel was obtained by setting a threshold midway between the open and closed levels and calculating the sum of open times and closed times.

The average results in this text are given as means ± S.E.M.

RESULTS

Resting potential of EE cells

The resting potential (V_r) of EE cells was measured in the current clamp mode of the perforated-patch method. In the control Tyrode solution, EE cells showed an average resting potential of −44·4 ± 0·8 mV ($n = 118$) in the intact small tissue preparations and −42·6 ± 3·0 mV ($n = 8$) in the cells isolated by the stamp method. These values are quite comparable to those observed in intact endothelial cells from coronary artery (−44·7 ± 0·24 mV; Chen & Cheung, 1992), and are slightly lower than those reported in intact aortic endothelial cells (−58 ± 8 mV; Marchenko & Sage, 1993). Oscillations in the membrane potential as demonstrated in the intact aortic endothelium (Marchenko & Sage, 1993) were scarcely observed. Resting potentials measured in the small tissue preparations from different cardiac chambers were quite comparable: right atrium, −46·2 ± 1·3 mV, $n = 55$; left atrium, −41·9 ± 1·4 mV, $n = 38$; tricuspid valve, −43·1 ± 2·0 mV, $n = 18$; mitral valve, −46·7 ± 3·3 mV, $n = 7$. It was difficult to measure the resting potential of the endothelial cells from either ventricle.

Effects of vasoactive substances on the membrane potential

Figure 1*A* shows representative records of transient hyperpolarizations induced by various vasoactive substances in small tissue preparations. Since the dose–response relationship was unavailable, concentrations of agonists were chosen to facilitate the comparison of the responses with those of cardiac microvascular endothelial cells (for example see Mehrke *et al.* 1991). Application of the agonists at the inlet of the recording chamber is indicated above each record. The delayed onset of the response was largely due to the time required for drug delivery, and the same delay was expected for wash-out. The peak amplitudes of the hyperpolarization induced by 10 μM ATP, 10 μM ADP, 10 μM AMP, 10 μM adenosine, 10 μM histamine and 1 μM substance P were 22·0 ± 1·0 ($n = 33$), 21·4 ± 2·0 ($n = 15$), 9·0 ± 2·1 ($n = 4$), 9·5 ± 1·3 ($n = 3$), 22·7 ± 1·6 ($n = 19$) and 14·6 ± 2·7 mV ($n = 6$), respectively (Table 1). In most cases, small fluctuations were observed in the membrane potential during the recovering phase.

Table 1 summarizes the agonist selectivity of EE cells. The response was regarded as positive when the membrane potential was hyperpolarized by more than 5 mV and recovered afterwards. The rate of observation of the response (Appearance, Table 1) varied among vasoactive substances. Almost 100% of preparations responded to ATP, ADP and histamine while responses to AMP or adenosine appeared only in 20–30% of the preparations. Whenever the response to AMP, adenosine or substance P was absent, the intactness of the ATP response was confirmed in the same preparation. In contrast to the results obtained in vascular endothelial cells (Mehrke *et al.*

1991; Chen & Cheung, 1992; Marchenko & Sage, 1993), no significant changes in the membrane potential were elicited by 1–200 μM ACh ($n = 6$), 0·05–5 μM bradykinin ($n = 5$) and 2 units ml^{-1} thrombin ($n = 5$). We also examined the effects of vasoactive substances known to affect the myocardial performance via the endocardium (Meulemans *et al.* 1988; Shah *et al.* 1989*a*; Schoemaker *et al.* 1990; Smith *et al.* 1991). Among such substances, only substance P induced hyperpolarization and no effects could be observed in 0·1 μM ANP ($n = 6$), 0·1 μM vasopressin ($n = 6$) or 10 μM serotonin ($n = 5$).

The response to substance P rapidly decayed as shown in Fig. 1*A*. Similar but delayed spontaneous decay was also observed during a longer application of ATP and histamine as shown in Fig. 1*B*. The late depolarization beyond the resting level, observed in coronary endothelium (Mehrke & Daut, 1990), was scarcely recorded in this study. If the duration of the hyperpolarizing response was measured from the onset of hyperpolarization to the time when the membrane potential reached either the control level or a new stable level, the duration was 62·6 ± 8·4 ($n = 8$) and 78·7 ± 25·0 s

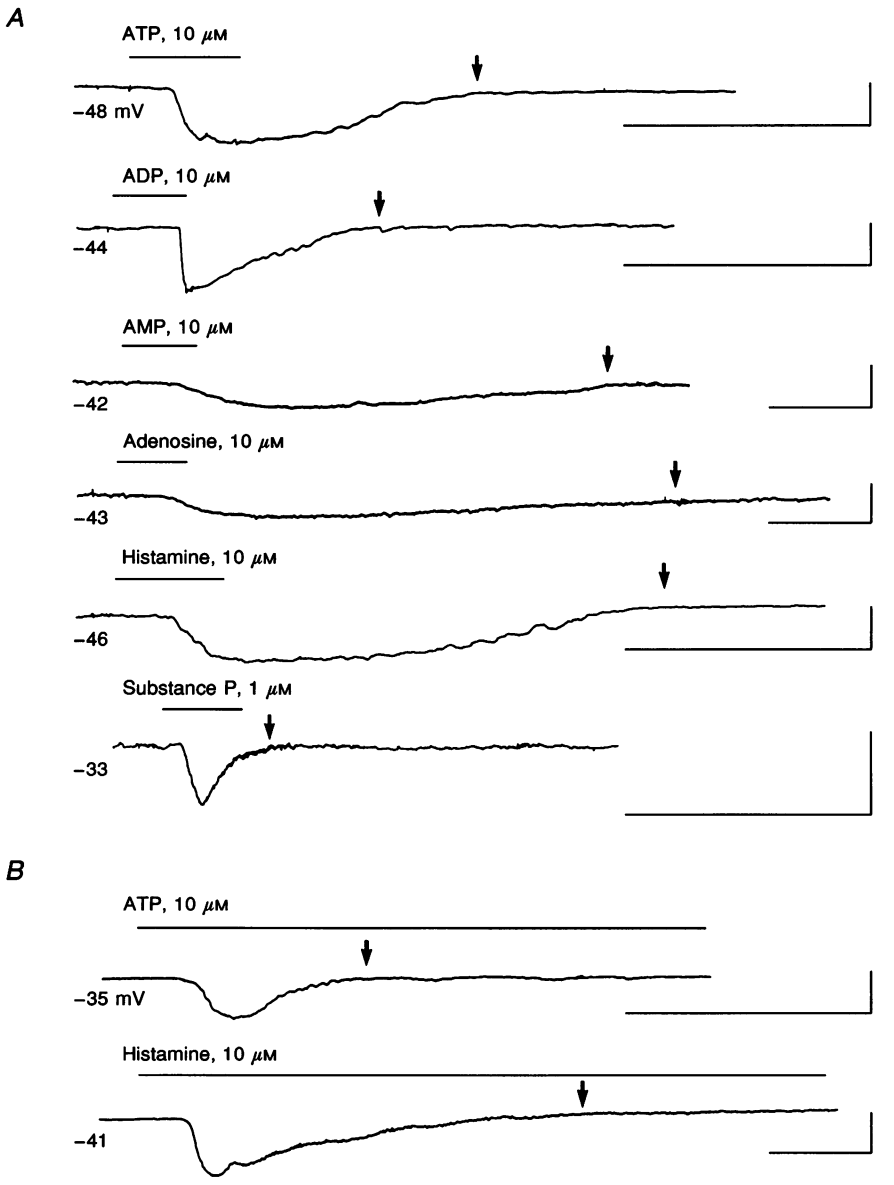

Figure 1. Hyperpolarization of EE cells induced by various vasoactive substances

The membrane potential was measured by perforated-patch recording in the small tissue preparation dissected from the atrial wall. The application of the agonists is indicated by the horizontal line. Each response was obtained from different preparations. The membrane potential before agonist application is indicated at the lower-left of each record. The arrow indicates the end of the hyperpolarizing response determined by eye. Vertical scale indicates 20 mV and horizontal scale 1 min in all cases. The records in *B* show responses to continuous application of ATP or histamine in the same preparation.

Table 1. Effects of vasoactive substances on the membrane potential

Agonist	Concentration	Hyperpolarization peak amplitude (mV)	Appearance (%)
ATP	10 μM	22·0 ± 1·0	80·5 (33/41)
ADP	10 μM	21·4 ± 2·0	100·0 (15/15)
AMP	10 μM	9·0 ± 2·1	23·5 (4/17)
Adenosine	10 μM	9·5 ± 1·3	30·0 (3/10)
Histamine	10 μM	22·7 ± 1·6	90·5 (19/21)
Substance P	1 μM	14·6 ± 2·7	50·0 (6/12)
ACh	1–200 μM	—	0 (0/6)
Bradykinin	0·05–5 μM	—	0 (0/5)
Thrombin	2 units ml^{-1}	—	0 (0/5)
ANP	0·1 μM	—	0 (0/6)
Vasopressin	0·1 μM	—	0 (0/6)
Serotonin	10 μM	—	0 (0/5)

Number of experiments in parentheses.

($n = 5$) for the ATP and histamine responses, respectively. The peak amplitudes of 20·3 ± 1·6 ($n = 8$, ATP) and 21·1 ± 3·9 mV ($n = 5$, histamine) were quite similar to those in the transient application (Fig. 1*A*). The results in Fig. 1*A* may indicate that effects of AMP and adenosine are weak but long lasting, as was described for coronary endothelial cells (Mehrke & Daut, 1990).

To identify the subtype of histaminergic receptors, we examined the effects of specific blockers. In Fig. 2*B*, an H_2 blocker, cimetidine (100 μM) was applied prior to the histamine application. The amplitude and duration of the histamine-induced hyperpolarization were quite similar to those of the control responses, which were recorded before and after the test run. On the other hand, 10 μM diphenhydramine, an H_1 blocker, blocked the histamine response (Fig. 2*A*). We failed to reverse the effect of diphenhydramine by washing for up to 20 min. In these experiments, histamine was applied at intervals of more than 5 min to allow recovery from the previous response. Essentially the same findings were obtained in six and four experiments for cimetidine and diphenhydramine, respectively. Thus, it was concluded that the action of histamine was mediated by an H_1 receptor. The purinergic receptor antagonist theophylline (50 μM) partially inhibited the responses to both ATP and adenosine (not shown, 11 experiments), but we failed to distinguish the receptor subtype.

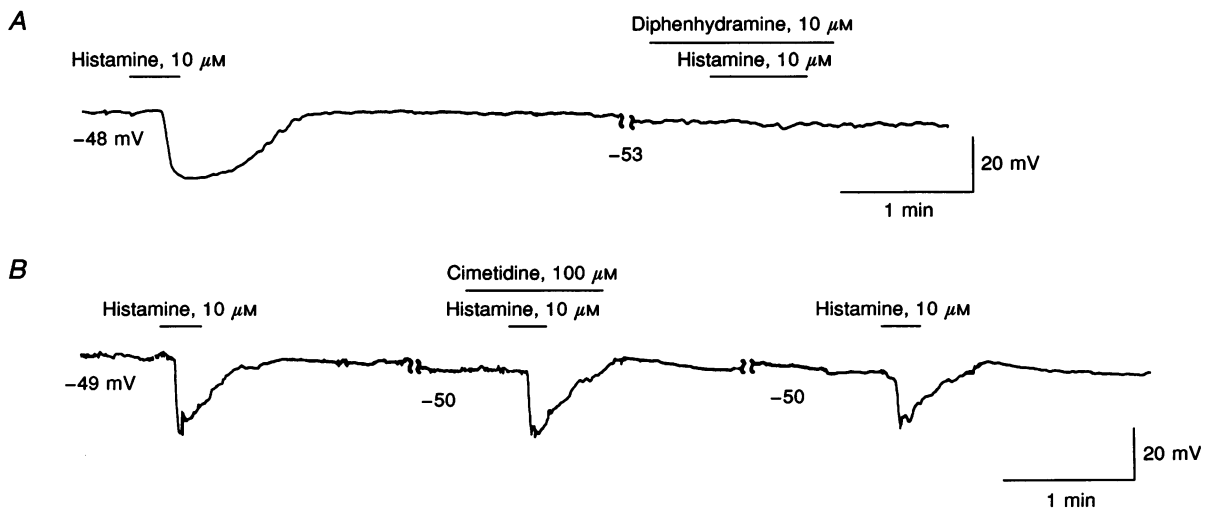

Figure 2. Effects of H_1 (*A*) and H_2 (*B*) histaminergic blockers

The period of time for the interruption (in each record) is 4–6 min which is long enough for the receptors to recover from desensitization as is evident in *B*.

Increase of the membrane K^+ conductance underlying the hyperpolarizing response

The membrane current induced by ATP and histamine was examined by whole-cell voltage clamp of cell clusters dissociated by the stream method. In the absence of agonists, the EE cells showed no obvious time-dependent currents during voltage jumps ($n = 18$). The application of 10 μM ATP shifted the holding current at −50 mV in the outward direction (Fig. 3). This ATP-induced outward current showed irregular fluctuations, most probably due to oscillations in the intracellular Ca^{2+} concentration. The concentration of EGTA in the pipette solution was 0·05 mM. To examine the time and voltage dependence of the ATP-induced current, the test voltage pulses were repeated in the presence of ATP, and the ATP-induced currents at various potentials were obtained by subtracting corresponding control currents (Fig. 3*B*). Although the holding current level fluctuated, it is evident that the ATP-induced current is virtually time independent over the potential range of −150 to +50 mV. The reversal potential of the ATP-induced current was around −80 mV (not shown). Essentially the same results were obtained in nine experiments.

To measure the *I–V* relationship without interference from the spontaneous decay of the response magnitude, ramp pulses were applied while monitoring the current change on the chart recorder. In the control external solution with 5·4 mM K^+, the application of ATP evoked a transient outward shift of the holding current at −50 mV (Fig. 4*A*). Figure 4*B* shows *I–V* relationships obtained at the peak and half-decayed responses in addition to the pre- and post-controls recorded at times indicated in Fig. 4*A*. The slope conductance, measured at −50 mV, increased from 14·7 to 172·2 pS pF^{-1} at the peak. The ATP-induced currents obtained by subtracting the pre-control from the peak (○ − ●) and from the half-response

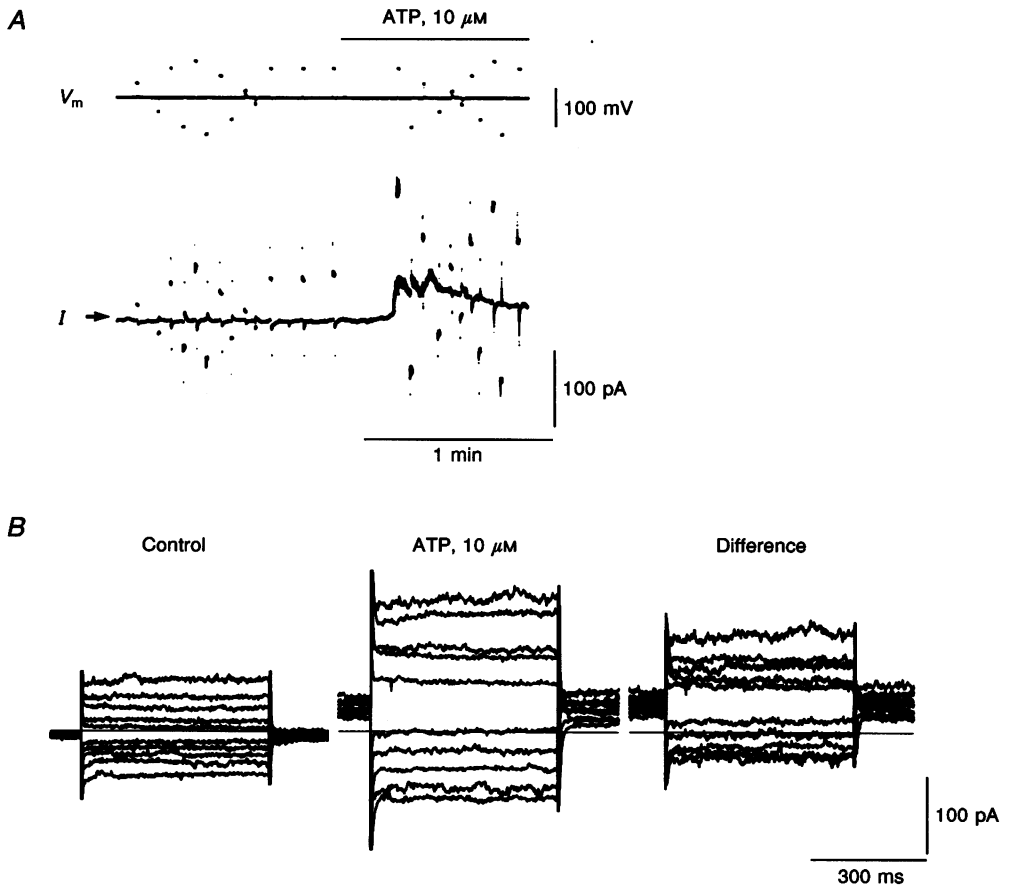

Figure 3. ATP-induced current measured by the square pulse protocol obtained in paired cells

A, the upper panel shows the membrane potential (V_m) and the lower panel the membrane current (I). The arrow indicates the zero-current level. The period of the ATP application is indicated by the horizontal line. Square pulses of 500 ms duration were applied over a range of −150 to +50 mV in 20 mV steps from a holding potential of −50 mV. *B*, current traces obtained in the control and during the ATP response are shown. The ATP-induced currents at various potentials (Difference) were obtained by subtracting corresponding control currents from those during the response. Horizontal lines indicate the zero-current level.

(■ – ●) reversed at −71·0 and −72·3 mV, respectively. Usually no significant shift of the reversal potential was detected during the time course of the ATP response. In the average of twenty-five experiments, the increase of the slope conductance measured at −50 mV was 94·9 ± 14·3 pS pF^{-1} and the difference current reversed at −73·3 ± 1·3 mV (Fig. 4*B*).

In the experiment shown in Fig. 5, the effect of changing external K^+ concentration ($[K^+]_o$) on the reversal potential of the ATP-induced current was examined. Increasing $[K^+]_o$ from 5·4 to 20 mM in the presence of ATP resulted in the inward shift of the holding current, maintaining the increased membrane conductance (Fig. 5*A*). The reversal potentials at 5·4 and 20 mM $[K^+]_o$ were measured by subtracting the control *I–V* relationship obtained at the corresponding $[K^+]_o$ as shown in Fig. 5*B*. The reversal potentials of ATP-induced current were −69 and −43 mV at 5·4 and 20 mM $[K^+]_o$, respectively. In seven experiments, the reversal potential was −72·2 ± 2·1 mV at 5·4 mM $[K^+]_o$ and −44·8 ± 2·9 mV at 20 mM $[K^+]_o$. This voltage shift of the reversal potential is slightly smaller than the theoretical shift of +34·4 mV of the K^+ equilibrium potential (E_K), and gives a permeability ratio, P_{Na}/P_K, of 0·019.

The histamine-induced current was also virtually time independent as examined by the square pulse protocol (not shown, $n = 6$). The *I–V* characteristics were examined by the ramp pulse protocol (Fig. 6). In thirteen experiments, the slope conductance of the histamine-induced current at −50 mV was 85·8 ± 17·4 pS pF^{-1} and

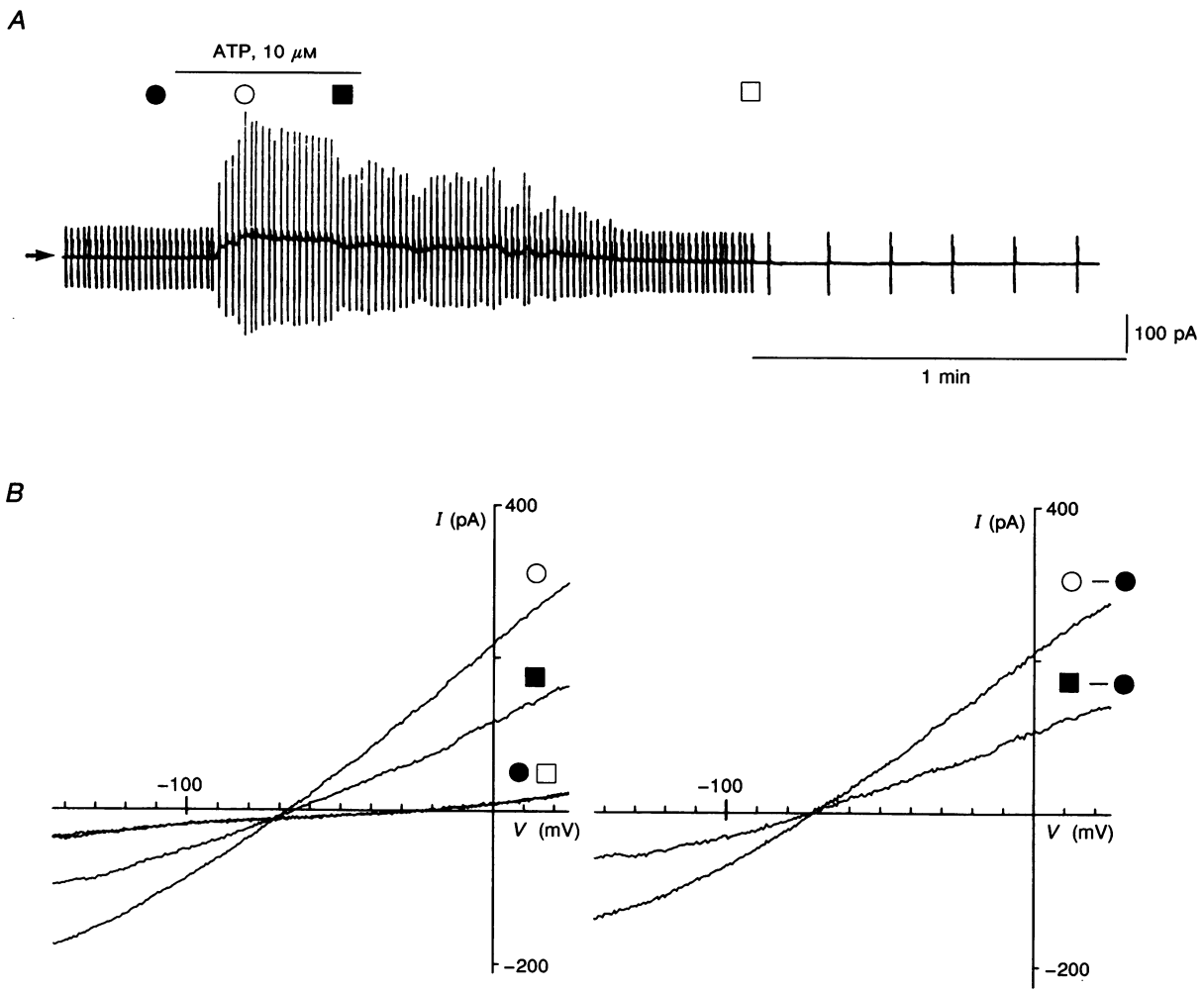

Figure 4. *I–V* characteristics of the ATP-induced current

A, a chart recording of the whole-cell current in triplet cells. Ramp pulses of ±100 mV were applied from a holding potential of −50 mV (d*V*/d*t*, ±2 V s^{-1}). The bath was perfused with the control Tyrode solution. The period of the ATP application is indicated by the horizontal line. The arrow indicates the zero-current level. *B*, *I–V* relationships were obtained at times indicated by corresponding symbols in *A*. The difference currents are shown in the right panel. The amplitude of vertical deflection in the chart recording (*A*) is larger than that illustrated in the *I–V* diagrams in *B* due to capacitive transient (2 C_m d*V*/d*t*).

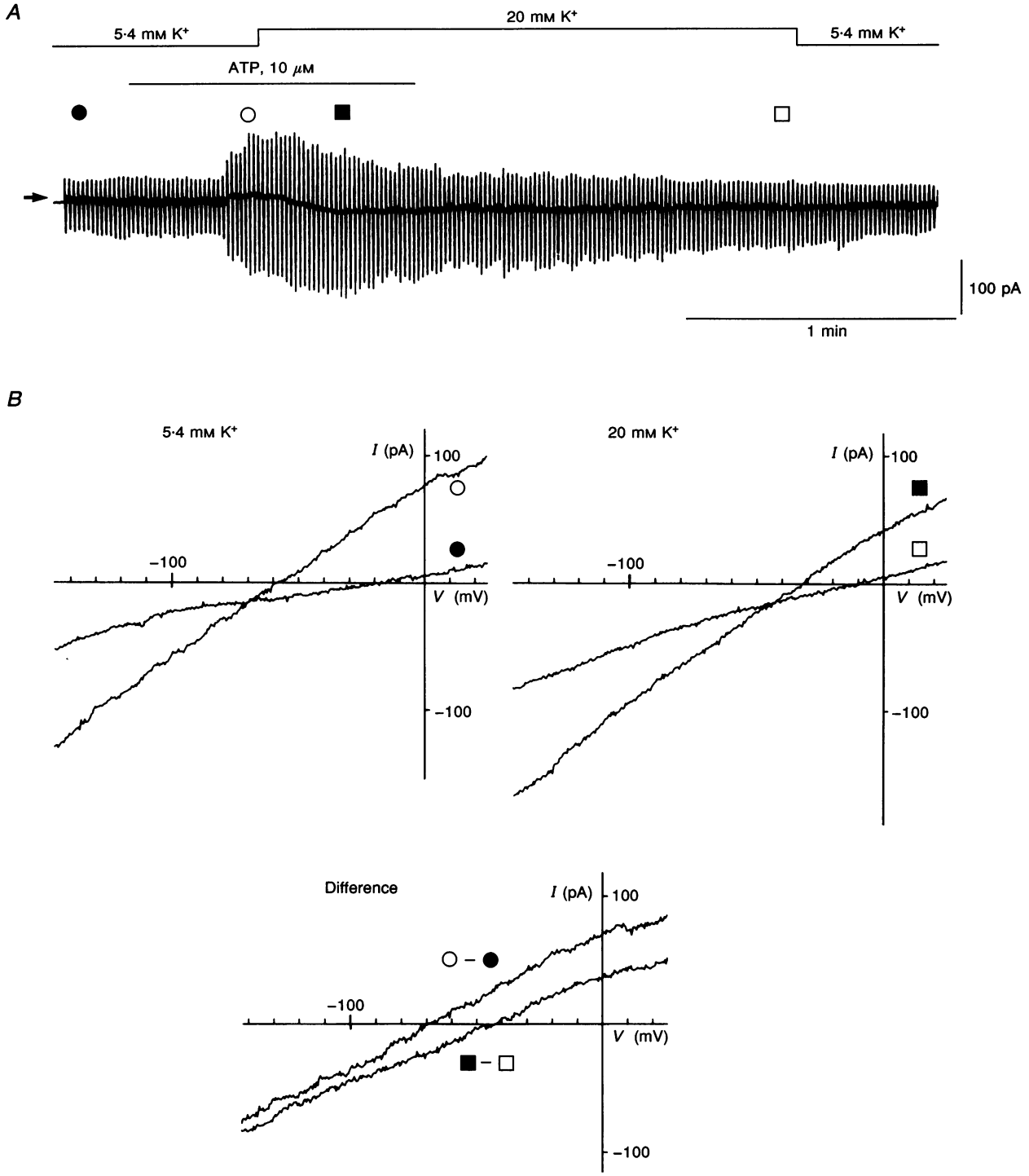

Figure 5. Reversal potential of ATP-induced currents at 5·4 and 20 mM $[K^+]_o$

A, a chart recording of the whole-cell current obtained from a single cell. Ramp pulses of ±100 mV were repeated from a holding potential of −50 mV (dV/dt, ±1 V s^{-1}), and $[K^+]_o$ was changed as indicated above the trace. The period of the ATP application is indicated by the horizontal line. The arrow indicates the zero-current level. *B*, *I–V* relationships obtained at the points indicated by corresponding symbols in *A*. *I–V* curves during the control (●) and the response (○) at 5·4 mM K^+ or those during the response (■) and after the recovery (□) at 20 mM K^+ are superimposed. *I–V* relationships for the difference currents at 5·4 mM K^+ (○ − ●) and 20 mM K^+ (■ − □) are also shown.

the reversal potential was $-73{\cdot}4 \pm 2{\cdot}1$ mV at 5·4 mM $[K^+]_o$. The reversal potentials remained stable throughout the course of most experiments. We conclude that both ATP- and histamine-induced currents are K^+ selective.

The ATP-induced current was observed in about half of the clusters of one to three cells (25/47 experiments) with 0·05 mM EGTA in the pipette solution. When the intracellular Ca^{2+} was buffered further with 10 mM EGTA, the current was observed in only two of thirty-nine experiments. Similarly, the success rate of observing histamine responses was markedly reduced from 41·9 (13/31) to 0% (0/21) by increasing EGTA in the pipette from 0·05 to 10 mM. Taken together, these results strongly suggest that the agonist-induced current is due to the activation of Ca^{2+}-dependent K^+ channels.

The *I–V* curve under the control conditions showed a slight inward rectification on hyperpolarization beyond −80 mV and a weak outward rectification at positive potentials. When $[K^+]_o$ was increased from 5·4 to 20 mM, the inward rectification on hyperpolarization was observed at less negative potentials and was enhanced (Fig. 5*B*). This finding suggests the presence of the inward rectifier K^+ current (see the accompanying paper, Manabe *et al.* 1995). Under the control conditions, the slope conductance at −50 mV was $290{\cdot}1 \pm 25{\cdot}5$ ($n = 25$), $300{\cdot}3 \pm 31{\cdot}0$ ($n = 23$) and $517{\cdot}0 \pm 36{\cdot}6$ pS ($n = 18$) for single, paired and triplet cells, respectively. The zero-current potential was less negative than the resting potential of the intact endothelium, and was $-29{\cdot}0 \pm 1{\cdot}2$ mV ($n = 66$) with 0·05 mM EGTA and $-9{\cdot}9 \pm 1{\cdot}8$ mV ($n = 41$) with 10 mM EGTA in the pipette. This finding may suggest a contribution of Ca^{2+}-dependent K^+ conductance to the resting potential (see the accompanying paper, Manabe *et al.* 1995).

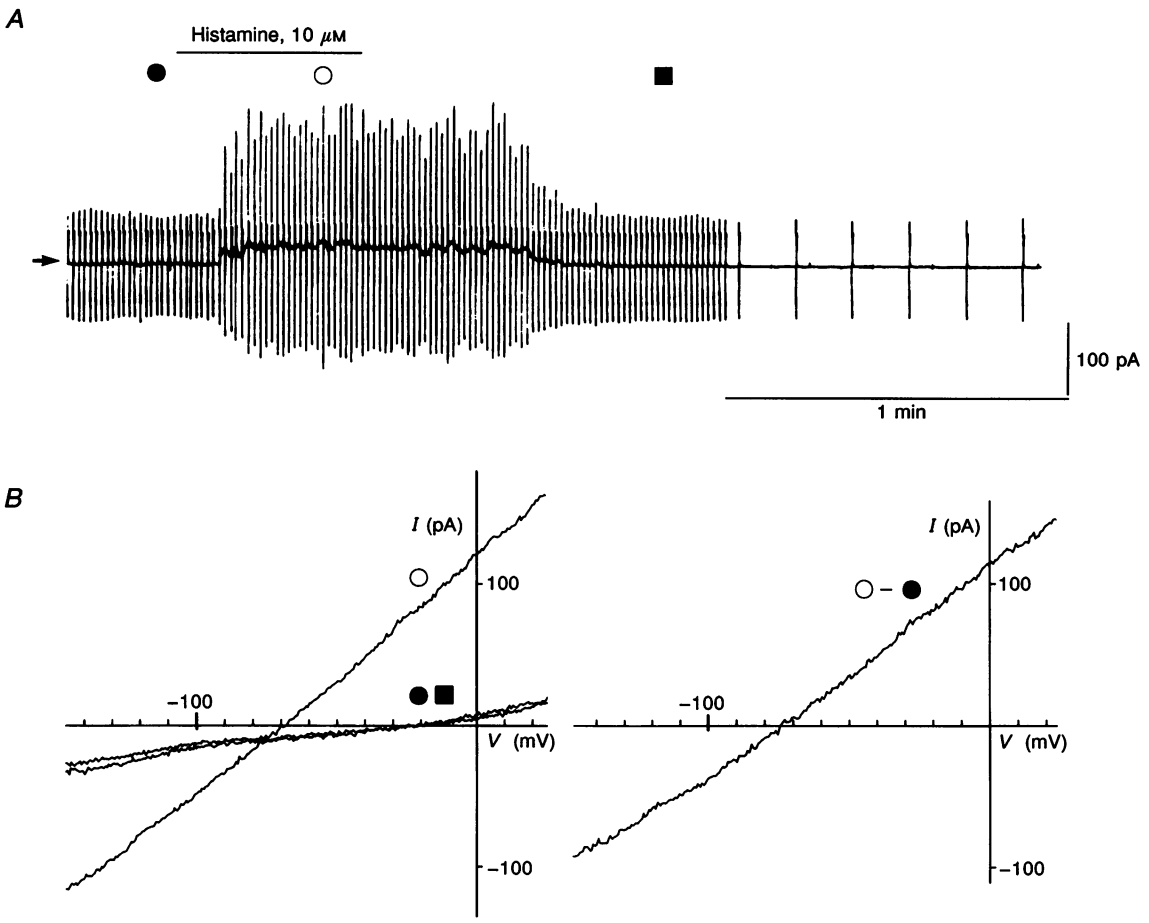

Figure 6. The *I–V* characteristics of the histamine-induced current

A, chart recording of the whole-cell current in triplet cells. Ramp pulses of ±100 mV were applied from a holding potential of −50 mV (dV/dt, ± 2 V s^{-1}). The bath was perfused with the control Tyrode solution. The period of the histamine application is indicated by the horizontal line. The arrow indicates the zero-current level. *B*, *I–V* relationships obtained at the times indicated by corresponding symbols in *A*. The difference current (○ − ●) is shown in the right panel.

During several experiments, the reversal potential of the ATP- or histamine-induced current gradually shifted in the positive direction. These experiments were not included in the analysis described above, and the positive shift might be explained by assuming an activation of additional ion channels other than the K^+ channel, such as the non-selective cation channel described in vascular endothelial cells (Mendelowitz *et al.* 1992; Nilius, Droogmans, Gericke & Schwarz, 1993). Separation of these minor components from the dominant K^+ current in the agonist-induced current is beyond the scope of the present study.

Single ionic channels responsible for the agonist-induced K^+ conductance

In vascular endothelial cells, it has been demonstrated that the extracellular application of ATP increases intracellular Ca^{2+} (Lückhoff & Busse, 1986; Ryan, Avdonin, Posin, Popov, Danilov & Tkachuk, 1988) and results in the activation of Ca^{2+}-dependent K^+ channels (Sauve, Parent, Simoneau & Roy, 1988; Mehrke & Daut, 1990; Vaca, Schilling & Kunze, 1992). A similar mechanism was suggested for the response of cultured bovine atrial EE cells to bradykinin (Laskey, Adams, Johns, Rubanyi & van Breemen, 1990). To search for K^+ channels, single channel currents were recorded using the high-K^+ pipette solution in the cell-attached mode from either the small tissue preparation or the cells obtained with the stamp method. The application of ATP to the bath successfully activated K^+ channels in five of more than eighteen patches (3 from the luminal membrane, and 2 from the abluminal membrane). The record in Fig. 7*A* was obtained from the luminal membrane and that in Fig. 7*B* was from the abluminal membrane. The response spontaneously decayed within 1 min even during the continuous application of ATP (Fig. 7*B*).

Figure 8 shows the current records at different voltages. The *I–V* relationship shows an inward rectification (Fig. 8*B*) with a slope conductance of $29{\cdot}5 \pm 2{\cdot}0$ pS ($n = 4$) measured at $V_r - 60$ mV. The zero-current potential may be 20–30 mV more positive to the resting potential. This value is near the expected E_K. In this experiment the channel activity was continuously recorded after the patch membrane was excised in the

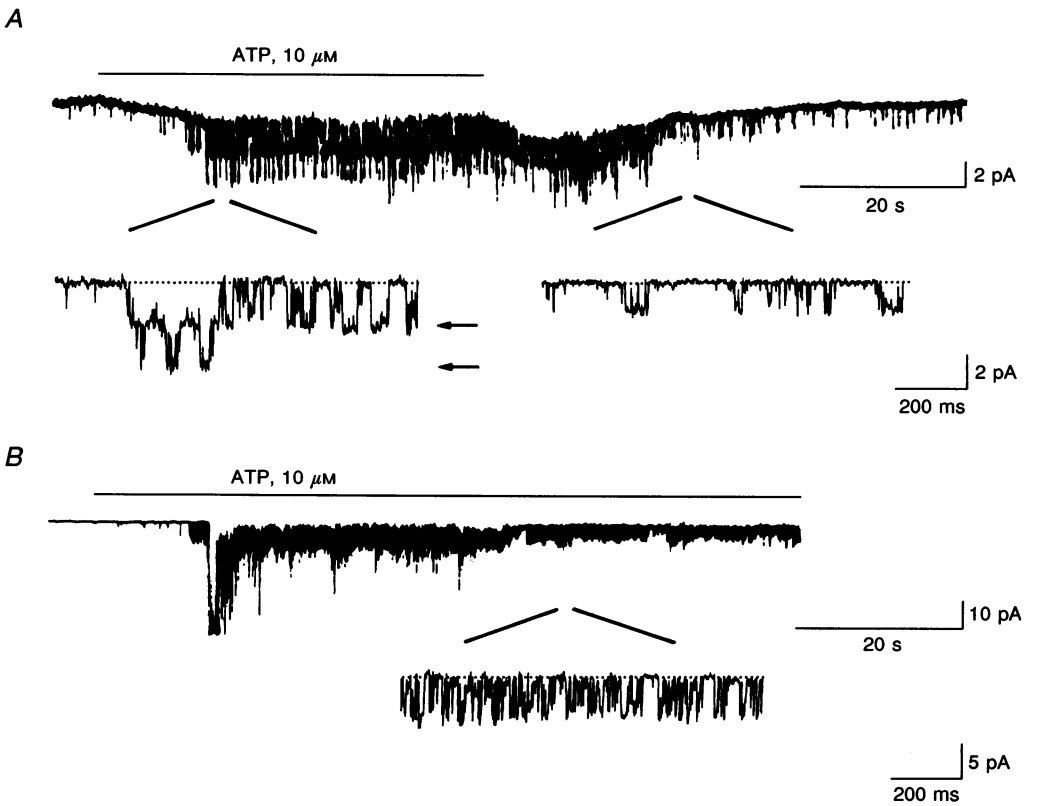

Figure 7. Single channel currents induced by 10 μM ATP in the cell-attached patch in the small tissue preparation (*A*) and in a cluster of cells isolated by the stamp method (*B*)

Time course of the response is illustrated by the chart recording, and individual events are shown on expanded scales. The application of 10 μM ATP is indicated by horizontal lines. The dotted lines indicate the closed levels. The pipette solution was the high-K^+ solution. *A*, holding potential, $V_r - 40$ mV. The different unit amplitudes between the two expanded traces are due to the change in the driving force during the hyperpolarization. The arrows indicate the open state levels. *B*, holding potential, $V_r - 120$ mV.

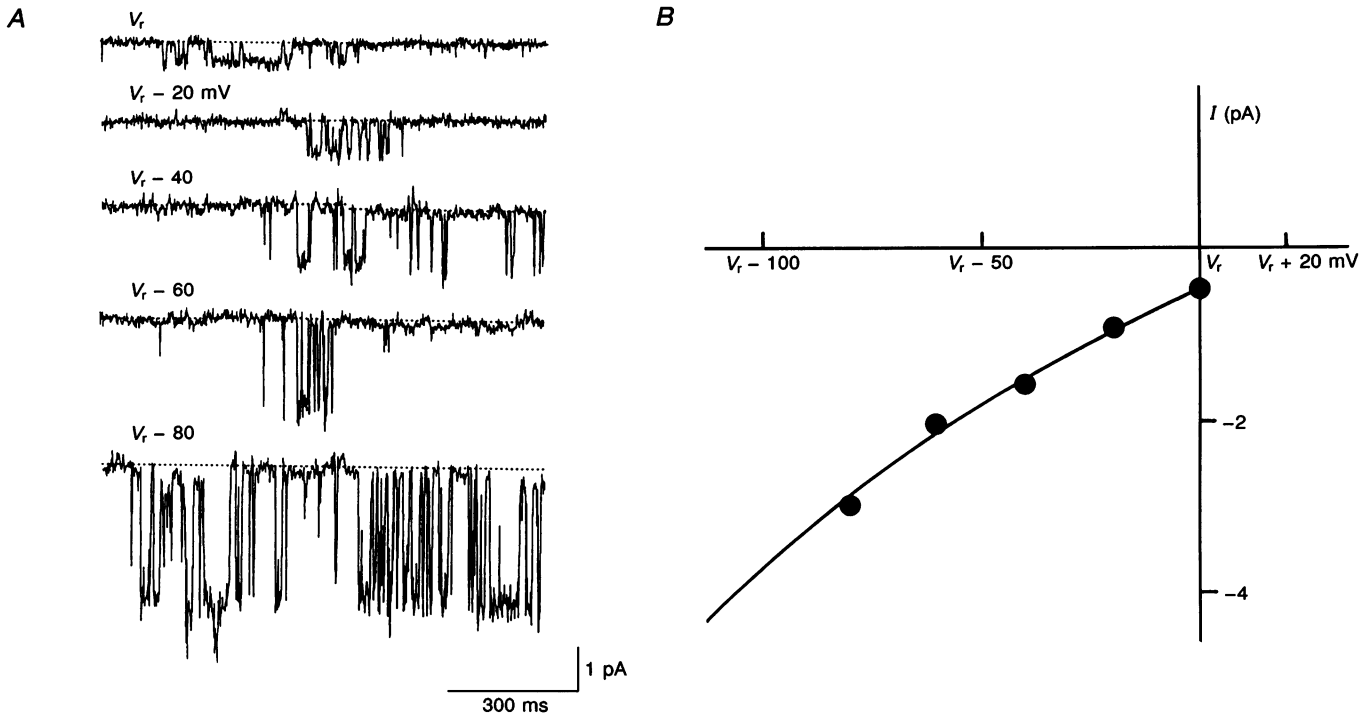

Figure 8. *I–V* relationship of the ATP-induced channel

A, cell-attached recordings of the ATP-induced channel in a cluster of cells isolated by the stamp method at different potentials. The records were obtained about 20 s after the onset of channel activation. The deviation from the resting potential is indicated at the upper-left of each trace. The dotted line indicates the closed level. *B*, *I–V* relationship of the channel shown in *A*. The slope conductance at $V_r - 60$ mV was 33 pS.

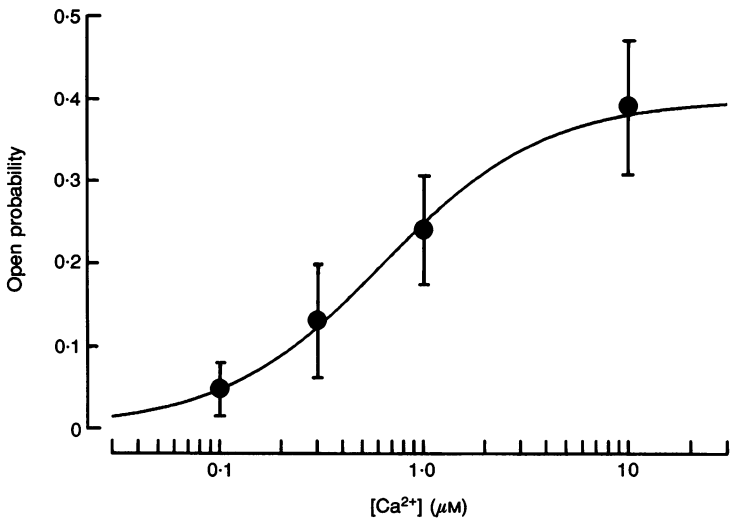

Figure 9. Ca^{2+} dependence of the 34 pS K^+ channel activity observed in inside-out patches of the luminal membrane

The mean ± S.E.M. ($n = 5$) of the open probability was plotted against different internal Ca^{2+} concentrations. The bath was perfused with 150 mM KCl solutions containing 0·1–10 μM Ca^{2+}. The Ca^{2+}-free 150 mM KCl solution with 0·3 or 1 mM EGTA was perfused and complete closure of the channel was confirmed before applying each Ca^{2+}-containing solution. The data points were fitted by the Hill equation using a least-squares algorithm. The dissociation constant, K_D, was 0·63 μM and the Hill coefficient 1·08. Holding potential, −40 mV; pipette solution, high-K^+ solution.

control Tyrode solution. Consistent with the K^+ gradient of external 150, internal 5·4 mM, the outward current could not be observed, and the current was inward at 0 mV. This finding is inconsistent with a Cl^- or non-selective cation conductance. The channel is tentatively called the 34 pS K^+ channel according to the average conductance in the inside-out patch recordings (see below).

Activation of the 34 pS K^+ channel by internal Ca^{2+}

To confirm the presence of Ca^{2+}-activated K^+ channels, the patch membrane was excised and exposed to Ca^{2+}-containing solutions. In one experiment, a membrane patch was excised after recording the ATP response, and the Ca^{2+}-mediated activation of the 34 pS K^+ channel was confirmed in the same patch. In five experiments, inside-out patches from the luminal membrane were prepared without testing the response to ATP, and the open probability of the 34 pS K^+ channel at −40 mV was measured and plotted against the Ca^{2+} concentration (Fig. 9). The open probability of the channel increased with increasing Ca^{2+} concentration roughly according to the Hill equation with a slope factor of 1·08.

K^+ selectivity of the 34 pS Ca^{2+}-dependent channel

After confirming the Ca^{2+}-dependent activation of the 34 pS channel, the *I–V* curves were obtained at different internal K^+ concentrations. In the experiments shown in Fig. 10, the open events reversed near 0 mV at 150 mM K^+ concentration, while at 5·4 mM K^+, the current was still inward at +43 mV. The *I–V* relationship showed an inward rectification and the slope conductance at the

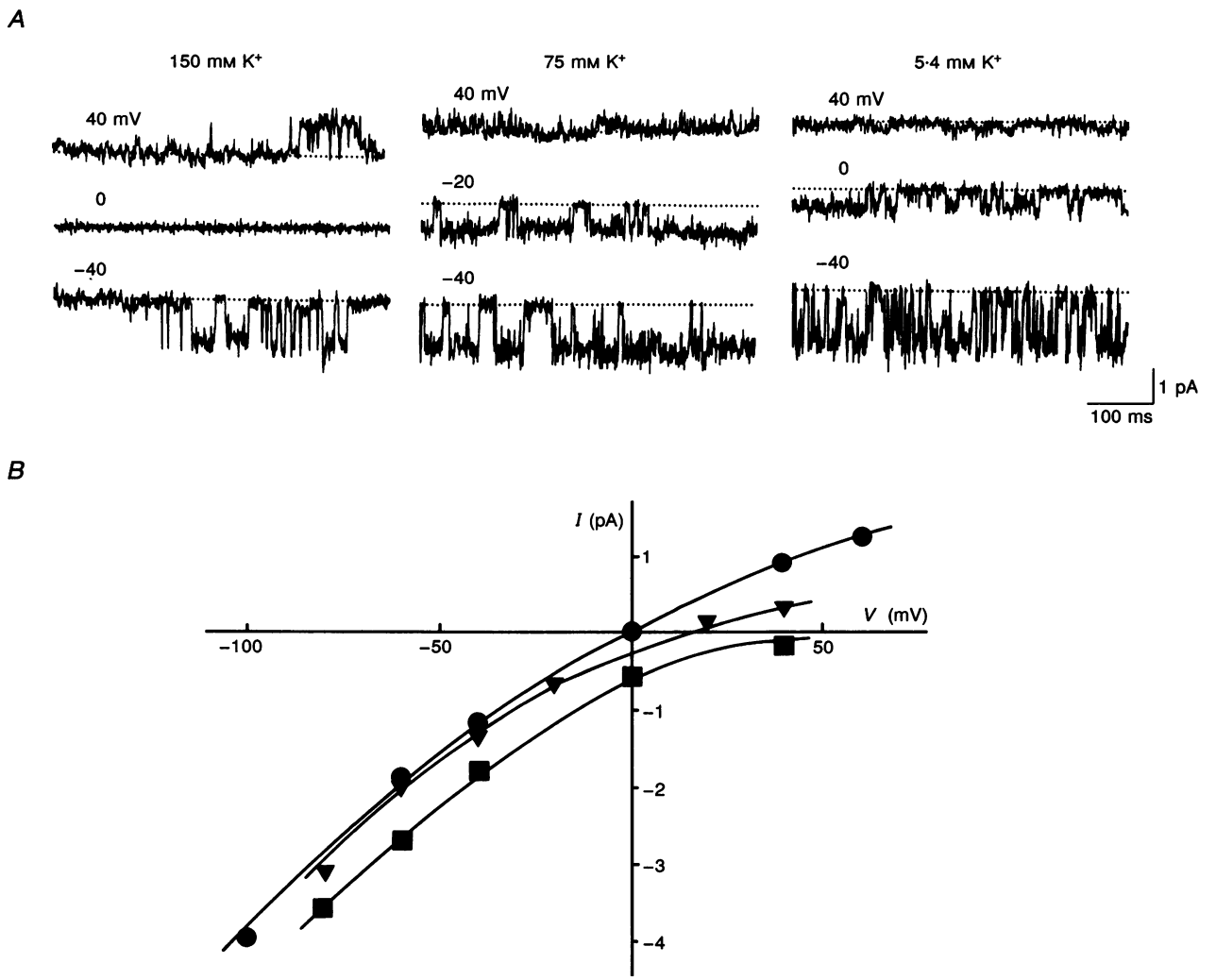

Figure 10. Inside-out recordings of the 34 pS channel at different internal K^+ concentrations

A, original current traces at the K^+ concentrations indicated. Na^+ was used to substitute for K^+ to maintain osmolarity. Each internal solution contained 10 μM Ca^{2+}. Different patches were used for each K^+ concentration. The data were filtered at 1 kHz and sampled at 2 kHz. The dotted lines indicate the closed level. *B*, *I–V* relationships of the channels shown in *A*. ●, 150 mM; ▼, 75 mM and ■, 5·4 mM K^+.

symmetrical 150 mM K^+ concentration was 33·5 ± 3·8 pS ($n = 4$). The reversal potential was measured as the intersection of the fitted smooth curve with the voltage axis as shown in Fig. 10. By reducing the internal K^+ concentration from 150 to 75 mM, the reversal potential shifted by 16·2 ± 0·5 mV ($n = 6$). The reversal potential at 5·4 mM K^+ was difficult to determine because of the strong inward rectification of the I–V curve. These findings are consistent with the K^+-sensitive nature of the 34 pS channel. No obvious change was observed in the open probability of the channel on voltage steps when activated with 1 μM Ca^{2+}: 0·34 ± 0·14 ($n = 3$), 0·24 ± 0·07 ($n = 5$), 0·30 ($n = 1$) and 0·25 ($n = 2$) at −80, −40, +40 and +80 mV, respectively, at the symmetrical 150 mM K^+ concentrations (not shown).

DISCUSSION

Comparison between the agonist-induced hyperpolarizations of EE cells and vascular endothelial cells

EE cells may share common roles with microvascular coronary endothelial cells both in the signal transduction from the circulating blood to the cardiac muscle cells and in the transepithelial exchange of various substances. Therefore, the comparison of the present experimental data with those reported in the coronary endothelial cells (Daut *et al.* 1988; Mehrke & Daut, 1990; Mehrke *et al.* 1991; Chen & Cheung, 1992) is of primary interest. The resting potential of these cells is relatively low compared with the aortic endothelial cells (Marchenko & Sage, 1993). Both types of the endothelial cells respond to ATP, adenosine and histamine with hyperpolarization in guinea-pig heart. However, in this study, EE cells did not respond to ACh, bradykinin or thrombin. Although, at present the physiological significance of this difference is not clear, the mechanisms underlying the hyperpolarizing responses might be comparable (see signal transduction pathway in vascular endothelial cells: Adams, Barakeh, Laskey & van Breemen, 1989; Cannell & Sage, 1989; Newby & Henderson, 1990; Vaca *et al.* 1992). In fact, a similar response of intracellular Ca^{2+} concentration was also demonstrated in cultured atrial EE cells (Laskey *et al.* 1990).

Although the peak amplitude of the hyperpolarization (>20 mV) was quite comparable to those reported in vascular endothelial cells (Chen & Cheung, 1992; Marchenko & Sage, 1993), the hyperpolarizing response induced by continuous application of ATP or histamine subsided within a few minutes in the EE cells. This response duration is considerably shorter than the sustained hyperpolarization observed in the confluent bovine aortic endothelial cells (Mehrke *et al.* 1991) or the initial hyperpolarizing phase of the ACh-induced response in the intact aortic endothelium (Marchenko & Sage, 1993). It is interesting that microvascular coronary endothelial cells showed a similar duration of responses to that of EE cells (Mehrke & Daut, 1990). This duration is rather similar to that recorded in the absence of the external Ca^{2+} in aortic endothelial cells (Mehrke *et al.* 1991; Marchenko & Sage, 1993), where the hyperpolarization was only due to the release of Ca^{2+} from intracellular stores. Further study on pathways for transmembrane Ca^{2+} influx is awaited in EE cells.

Types and distribution of the receptors in EE cells

Many studies have reported the response to vasoactive substances in vascular endothelial cells. There seems to be some discrepancy between the results from cultured endothelial cells even from the same organ. For example, the effects of ACh in cultured aortic endothelial cells are not consistent (Olesen, Davies & Clapham, 1988; Mehrke *et al.* 1991). This finding has been attributed to a rapid loss of ACh receptors in some culture conditions (Tracey & Peach, 1992), emphasizing the importance of using intact preparations. Using the intact EE cells, we demonstrate for the first time that purinergic agonists (ATP, ADP, AMP and adenosine), histamine and substance P induce hyperpolarization. ACh and bradykinin, which have been reported to hyperpolarize the membrane in aortic and/or coronary endothelial cells (Chen & Cheung, 1992; Marchenko & Sage, 1993) had no effect on EE cells. This finding may contrast with a recent report showing a transient increase in the intracellular Ca^{2+} concentration caused by ACh in endocardial cells of rabbit pulmonary and aortic valves (Laskey, Adams & van Breemen, 1994).

The histaminergic receptor was pharmacologically identified to be an H_1 type in the present study. Although we did not examine various selective blockers for the subtypes of purinergic receptor, the different time courses of the responses (Fig. 1*A*) may indicate a different subtype of the receptor for adenosine and AMP from that for ATP and ADP. This view is supported by the large difference in the success rates of observing the responses (Table 1). The responses to ATP and ADP were observed in most of the small tissue preparations, while those to adenosine and AMP were observed in only 20–30% of the preparations. Essentially the same findings were reported for microvascular coronary endothelial cells (Mehrke & Daut, 1990), where the response to adenosine was observed in only 58% of the monolayers studied while ATP always elicited the response. A result also similar to that in microvascular coronary endothelial cells is that EE cells have a relatively smaller and longer response to adenosine compared with ATP. Considering the electrical connections between cells, it may be speculated that receptors for AMP and adenosine (P_1-type of purinoceptors) and receptors for substance P are distributed in a mosaic manner in the monolayer of EE cells, and that cells in a given small area do not express a

given type of receptors, while the P_2-type of the purinergic receptors may be distributed homogeneously in both the coronary bed and EE cells. The finding that the ATP or histamine response was observed in about 50% of cells dissociated by the stream method might be due either to variable extents of chelation of the intracellular Ca^{2+} with 0·05 mM EGTA in the pipette solution, or to a real absence of the receptor in the cells used for voltage clamp.

The Ca^{2+}-activated K^+ channel

The whole-cell current analysis revealed that the ATP- and histamine-induced currents were K^+ selective (Figs 4–6) and were inhibited by increasing the intracellular Ca^{2+} buffer. The single channel recordings demonstrated the presence of the 34 pS K^+ channel (Fig. 10), which was activated by the internal application of Ca^{2+} (Fig. 9). These findings suggest that the 34 pS Ca^{2+}-activated K^+ channel is responsible for the ATP- or histamine-induced hyperpolarization. To conclude unequivocally the link between the ATP-activated single channel in the cell-attached patch (Figs 7 and 8) and the 34 pS Ca^{2+}-activated K^+ channel in the inside-out patch (Fig. 10), continuous recordings of cell-attached followed by the excised patch recordings will be required. With our present technique, such an extensive study was unrealistic.

The conductance and gating properties of the 34 pS K^+ channel are quite comparable to those of the Ca^{2+}-dependent K^+ channel activated by bradykinin in cultured bovine aortic endothelial cells (Vaca *et al.* 1992). The *I–V* curve showed a weak inward rectification with a limiting slope conductance of about 30 pS and the open probability was only weakly voltage dependent. Both channels were activated with a threshold Ca^{2+} concentration of 0·01 μM. The whole-cell K^+ current showed no significant time-dependent change with voltage steps (Fig. 3). Similar properties were also obtained in the bradykinin-activated K^+ channel, but the limiting slope conductance of 54·7 pS seems to be larger (Colden-Stanfield *et al.* 1992). Single channel recordings are still not available from microvascular coronary endothelial cells.

Another class of Ca^{2+}-dependent K^+ channel is presented in the accompanying paper (Manabe *et al.* 1995). This channel has a unitary conductance of 210 pS and requires a slightly higher intracellular Ca^{2+} concentration for its activation (0·3 μM, authors' unpublished observation). The agonist-induced current did not show large current noise on strong depolarization (Figs 3–6). However, taking the large conductance into account, the 210 pS channel may, in part, play a role in the agonist-induced hyperpolarization.

Physiological role of the agonist-induced hyperpolarization

ATP is known to be released from the sympathetic nerve terminals. In addition, platelet aggregation results in the release of several substances including ATP (Reimers, 1985). An ATP concentration of more than 10 μM produces a positive inotropic effect in the papillary muscle. This effect was accentuated by removing the EE cells, and it was suggested that the EE cells not only act as a physical barrier but also modulate the myocardial contractility by releasing an unknown chemical messenger (Shah, Meulemans & Brutsaert, 1989*b*). It is hypothesized that the hyperpolarization induced by the Ca^{2+} release from intracellular stores produces a further increase of the intracellular Ca^{2+} concentration by enhancing transmembrane Ca^{2+} influx through several pathways: the receptor-mediated pathway, Ca^{2+} leakage pathway and stretch-activated Ca^{2+} pathway (Johns, Lategan, Lodge, Ryan, van Breemen & Adams, 1987; Adams *et al.* 1989; Nilius *et al.* 1993). All of these pathways are reported to be non-selective for cations (Nilius *et al.* 1993). Hyperpolarization due to activation of the Ca^{2+}-activated K^+ channel may provide the electrochemical driving force for the transmembrane Ca^{2+} influx through these pathways (Laskey *et al.* 1990). The increase of intracellular Ca^{2+} may stimulate the secretion of chemical mediators (Lückhoff & Busse, 1990; Kukovetz, Graier & Groschner, 1992).

It has been reported that substance P (Smith *et al.* 1991), vasopressin (Schoemaker *et al.* 1990), serotonin (Shah *et al.* 1989*a*) and ANP (Meulemans *et al.* 1988; Smith *et al.* 1991) also produce negative inotropic effects in an endocardium-dependent manner. In the present study, substance P induced hyperpolarization in EE cells, while the other substances did not, even at the concentrations we consider to have been sufficiently high. We used mainly atrial EE cells, and we cannot exclude the possibility that ventricular EE cells might have a different set of receptors.

ADAMS, D. J., BARAKEH, J., LASKEY, R. & VAN BREEMEN, C. (1989). Ion channels and regulation of intracellular calcium in vascular endothelial cells. *FASEB Journal* **3**, 2389–2400.

BRUTSAERT, D. L. (1989). The endocardium. *Annual Review of Physiology* **51**, 263–273.

BRUTSAERT, D. L. & ANDRIES, L. J. (1992). The endocardial endothelium. *American Journal of Physiology* **263**, H985–1002.

CANNELL, M. B. & SAGE, S. O. (1989). Bradykinin-evoked changes in cytosolic calcium and membrane currents in cultured bovine pulmonary artery endothelial cells. *Journal of Physiology* **419**, 555–568.

CHEN, G. & CHEUNG, D. W. (1992). Characterization of acetylcholine-induced membrane hyperpolarization in endothelial cells. *Circulation Research* **70**, 257–263.

COLDEN-STANFIELD, M., CRAMER, E. B. & GALLIN, E. K. (1992). Comparison of apical and basal surfaces of confluent endothelial cells: patch-clamp and viral studies. *American Journal of Physiology* **263**, C573–583.

DAUT, J., MEHRKE, G., NEES, S. & NEWMAN, W. H. (1988). Passive electrical properties and electrogenic sodium transport of cultured guinea-pig coronary endothelial cells. *Journal of Physiology* **402**, 237–254.

FABIATO, M. & FABIATO, F. (1979). Calculator programs for computing the composition of the solutions containing multiple metals and ligands used for experiments in skinned muscle cells. *Journal de Physiologie* **75**, 463–505.

HAMILL, O. P., MARTY, A., NEHER, E., SAKMANN, B. & SIGWORTH, F. J. (1981). Improved patch-clamp techniques for high-resolution current recording from cells and cell-free membrane patches. *Pflügers Archiv* **391**, 85–100.

ITO, H., MATSUDA, H. & NOMA, A. (1993). Ion channels in the luminal membrane of endothelial cells of the bull-frog heart. *Japanese Journal of Physiology* **43**, 191–206.

JOHNS, A., LATEGAN, T. W., LODGE, N. J., RYAN, U. S., VAN BREEMEN, C. & ADAMS, D. J. (1987). Calcium entry through receptor-operated channels in bovine pulmonary artery endothelial cells. *Tissue and Cell* **19**, 733–745.

KUKOVETZ, W. R., GRAIER, W. F. & GROSCHNER, K. (1992). Contribution of agonist-induced hyperpolarization to Ca^{2+} influx and formation of EDRF in vascular endothelial cells. *Japanese Journal of Pharmacology* **58**, suppl. 2, 213–219P.

LASKEY, R. E., ADAMS, D. J., JOHNS, A., RUBANYI, G. M. & VAN BREEMEN, C. (1990). Membrane potential and Na^+–K^+ pump activity modulate resting and bradykinin-stimulated changes in cytosolic free calcium in cultured endothelial cells from bovine atria. *Journal of Biological Chemistry* **265**, 2613–2619.

LASKEY, R. E., ADAMS, D. J. & VAN BREEMEN, C. (1994). Cytosolic [Ca^{2+}] measurements in endothelium of rabbit cardiac valves using imaging fluorescence microscopy. *American Journal of Physiology* **266**, H2130–2135.

LÜCKHOFF, A. & BUSSE, R. (1986). Increased free calcium in endothelial cells under stimulation with adenine nucleotides. *Journal of Cellular Physiology* **126**, 414–420.

LÜCKHOFF, A. & BUSSE, R. (1990). Calcium influx into endothelial cells and formation of endothelium-derived relaxing factor is controlled by the membrane potential. *Pflügers Archiv* **416**, 305–311.

MANABE, K., ITO, H., MATSUDA, H., NOMA, A. & SHIBATA, Y. (1995). Classification of ion channels in the luminal and abluminal membranes of guinea-pig endocardial endothelial cells. *Journal of Physiology* **484**, 41–52.

MARCHENKO, S. M. & SAGE, S. O. (1993). Electrical properties of resting and acetylcholine-stimulated endothelium in intact rat aorta. *Journal of Physiology* **462**, 735–751.

MEBAZAA, A., MAYOUX, E., MAEDA, K., MARTIN, L. D., LAKATTA, E. G., ROBOTHAM, J. L. & SHAH, A. M. (1993). Paracrine effects of endocardial endothelial cells on myocyte contraction mediated via endothelin. *American Journal of Physiology* **265**, H1841–1846.

MEHRKE, G. & DAUT, J. (1990). The electrical response of cultured guinea-pig coronary endothelial cells to endothelium-dependent vasodilators. *Journal of Physiology* **430**, 251–272.

MEHRKE, G., POHL, U. & DAUT, J. (1991). Effects of vasoactive agonists on the membrane potential of cultured bovine aortic and guinea-pig coronary endothelium. *Journal of Physiology* **439**, 277–299.

MENDELOWITZ, D., BACAL, K. & KUNZE, D. L. (1992). Bradykinin-activated calcium influx pathway in bovine aortic endothelial cells. *American Journal of Physiology* **262**, H942–948.

MEULEMANS, A. L., SIPIDO, K. R., SYS, S. U. & BRUTSAERT, D. L. (1988). Atriopeptin III induces early relaxation of isolated mammalian papillary muscle. *Circulation Research* **62**, 1171–1174.

MISTRY, D. K. & HABLITZ, J. J. (1990). Nystatin-perforated patch recordings disclose NMDA-induced outward currents in cultured neocortical neurons. *Brain Research* **535**, 318–322.

NEWBY, A. C. & HENDERSON, A. H. (1990). Stimulus–secretion coupling in vascular endothelial cells. *Annual Review of Physiology* **52**, 661–674.

NILIUS, B., DROOGMANS, G., GERICKE, M. & SCHWARZ, G. (1993). Nonselective ion pathways in human endothelial cells. In *Nonselective Cation Channels: Pharmacology, Physiology and Biophysics*, ed. SIEMEN, D. & HESCHELER, J., pp. 269–280. Birkhauser Verlag, Basel, Switzerland.

OLESEN, S. P., DAVIES, P. F. & CLAPHAM, D. E. (1988). Muscarinic-activated K^+ current in bovine aortic endothelial cells. *Circulation Research* **62**, 1059–1064.

PATLAK, J. B. (1988). Sodium channel subconductance levels measured with a new variance–mean analysis. *Journal of General Physiology* **92**, 413–430.

REIMERS, H. J. (1985). Adenine nucleotides in blood platelets. In *The Platelets. Physiology and Pharmacology*, ed. LONGENECKER, G. L., pp. 85–112. Academic Press Inc., Orlando, FL, USA.

RYAN, U. S., AVDONIN, P. V., POSIN, E. Y., POPOV, E. G., DANILOV, S. M. & TKACHUK, V. A. (1988). Influence of vasoactive agents on cytoplasmic free calcium in vascular endothelial cells. *Journal of Applied Physiology* **65**, 2221–2227.

SAUVE, R., PARENT, L., SIMONEAU, C. & ROY, G. (1988). External ATP triggers a biphasic activation process of a calcium-dependent K^+ channel in cultured bovine aortic endothelial cells. *Pflügers Archiv* **412**, 469–481.

SCHOEMAKER, I. E., MEULEMANS, A. L., ANDRIES, L. J. & BRUTSAERT, D. L. (1990). Role of endocardial endothelium in positive inotropic action of vasopressin. *American Journal of Physiology* **259**, H1148–1151.

SHAH, A. M., ANDRIES, L. J., MEULEMANS, A. L. & BRUTSAERT, D. L. (1989*a*). Endocardium modulates myocardial inotropic response to 5-hydroxytryptamine. *American Journal of Physiology* **257**, H1790–1797.

SHAH, A. M., MEULEMANS, A. L. & BRUTSAERT, D. L. (1989*b*). Myocardial inotropic responses to aggregating platelets and modulation by the endocardium. *Circulation* **79**, 1315–1323.

SMITH, J. A., SHAH, A. M. & LEWIS, M. J. (1991). Factors released from endocardium of the ferret and pig modulate myocardial contraction. *Journal of Physiology* **439**, 1–14.

TAKEDA, K. & KLEPPER, M. (1990). Voltage-dependent and agonist-activated ionic currents in vascular endothelial cells: a review. *Blood Vessels* **27**, 169–183.

TRACEY, W. R. & PEACH, M. J. (1992). Differential muscarinic receptor mRNA expression by freshly isolated and cultured bovine aortic endothelial cells. *Circulation Research* **70**, 234–240.

Tsien, R. Y. & Rink, T. J. (1980). Neutral carrier ion-selective microelectrodes for measurement of intracellular free calcium. *Biochimica et Biophysica Acta* **599**, 623–638.

Vaca, L., Schilling, W. P. & Kunze, D. L. (1992). G-Protein-mediated regulation of a Ca^{2+}-dependent K^+ channel in cultured vascular endothelial cells. *Pflügers Archiv* **422**, 66–74.

Yamamoto, Y., Chen, G., Miwa, K. & Suzuki, H. (1992). Permeability and Mg^{2+} blockade of histamine-operated cation channel in endothelial cells of rat intrapulmonary artery. *Journal of Physiology* **450**, 395–408.

Wang, J. & Morgan, J. P. (1992). Endocardial endothelium modulates myofilament Ca^{2+} responsiveness in aequorin-loaded ferret myocardium. *Circulation Research* **70**, 754–760.

Acknowledgements

We thank Drs R. A. Barrett-Jolley, K. Ono and B. T. Quinn for reading the manuscript. We also thank Miho Fukushima for her secretarial assistance.

Author's present address

H. Matsuda: Department of Physiology, Kansai Medical University, Moriguchi, Osaka 570, Japan.

Received 25 January 1994; accepted 14 September 1994.